Crystallization and texturing in rapidly quenched $Nd_2Fe_{14}B_1$ and $Nd_{15}Fe_{77}B_8$

Guo-hau Tu,[a] Z. Altounian, D. H. Ryan, and J. O. Ström-Olsen
Rutherford Physics Building, McGill University, 3600 University Street, Montreal, Quebec, H3A 2T8, Canada

The crystallization and texturing in amorphous $Nd_2Fe_{14}B$ and $Nd_{15}Fe_{77}B_8$ were investigated. The crystallization kinetics for both compositions were similar with an activation energy of 3.5 eV, an Avrami exponent of 3.4, and crystallization enthalpy of 5.1 kJ/mol. Extreme texturing, with the *c* axis perpendicular to the ribbon plane, is observed in the slow quench materials. Similar, but less pronounced, effects are seen in the recrystallized alloys. In some cases surface oxidation was found to give the samples the appearance of texture due to a combination of Nd_2O_3 and alpha-iron reflections.

INTRODUCTION

Two methods exist for preparing Nd-Fe-B permanent magnet material by rapid quenching. The first, and more widely used, is to produce by relatively slow quench rates a microcrystalline material with good magnetic properties, which can further be improved by subsequent thermal treatment.[1] Alternatively the alloy may be rapidly quenched into the *amorphous state* and then crystallized by subsequent heat treatment to obtain the optimum magnetic performance.[2,3] For both procedures, the assesment of the composition and texture of the resultant materials is complicated by the formation of surface oxides during the production and treatment phases. Furthermore, problems arise in the second case from the difficulty of producing truly amorphous material. In this paper we present data on the crystallization and texturing of Nd-Fe-B alloys prepared by both methods.

EXPERIMENTAL METHODS

Alloys of the stoichiometric composition $Nd_2Fe_{14}B$ and the off-stoichiometric composition at $Nd_{15}Fe_{77}B_8$ were prepared by induction melting appropriate amounts of Nd (99.9%), Fe (99.99%), and B (99.9%) on a water-cooled copper boat under Ti-gettered argon. We find that this method yields much cleaner samples than conventional arc melting and leads to essentially no loss of constituents (less than 0.02% after 10 meltings). The alloys were melt spun on a steel wheel with tangential speeds of up to 45 m/s under high-purity argon. Inferior results were obtained with the more usual copper wheel (for which the contact time of the ribbon is too short) or by using a helium atmosphere. The crystallization characteristics were studied by differential scanning calorimetry (DSC), using a Perkin-Elmer DSC-2C and the surfaces of the recrystallized samples were examined using conversion electron Mössbauer spectroscopy (CEMS) which is sensitive to only the outer 100 nm of the sample. Ribbons were fixed to aluminum foil using conducting paint to form the cathode of a flowing gas proportional counter with a 5% methane/helium mixture to minimize the background due to x-ray and gamma-ray photons. Spectra were recorded on a conventional constant acceleration drive with a 1GBq ^{57}Fe *Pd* source.

[a] Permanent address: Dept. of Physics, Nanjing Normal University, Nanjing, China.

RESULTS AND DISCUSSION

Figure 1 shows the x-ray diffraction pattern of a typical amorphous ribbon of $Nd_2Fe_{14}B$ spun at 45 m/s. No contribution from crystalline phases is seen, even on long exposure from both the free and wheel surfaces of the ribbon. The Mössbauer spectrum (not shown) also indicates no crystallinity. Similar results are obtained for $Nd_{15}Fe_{77}B_8$. On crystallization, *a*-$Nd_2Fe_{14}B$ produces only $Nd_2Fe_{14}B$. The excess Nd and B in *a*-$Nd_{15}Fe_{77}B_8$ appear as $Nd_{1.1}Fe_4B_4$, which is seen only in transmission Mössbauer spectra, with, presumably, some free Nd. DSC isothermal data show that the kinetics of the crystallization are similar in both systems. Figure 2 shows Kissinger and Avrami plots for the two alloys.[4] Not only are the activation energies the same (3.5 ± 0.1 eV), but also the Avrami exponents are identical, 3.4 ± 0.1. These results suggest that crystallization proceeds by the same polymorphic reaction in the two alloys: diffusion-controlled growth with constant rate of nucleation. This suggests that crystallization with higher heating rates will produce a higher density of nuclei which are believed to be essential for the high coercivity in these materials. This is supported by our preliminary magnetic measurements. The

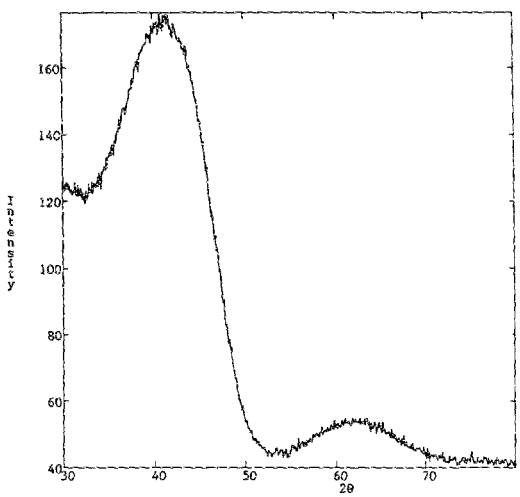

FIG. 1. X-ray diffraction scan for $Nd_2Fe_{14}B$ melt spun at 45 m/s showing only amorphous material.

 0021-8979/88/083330-03$02.40

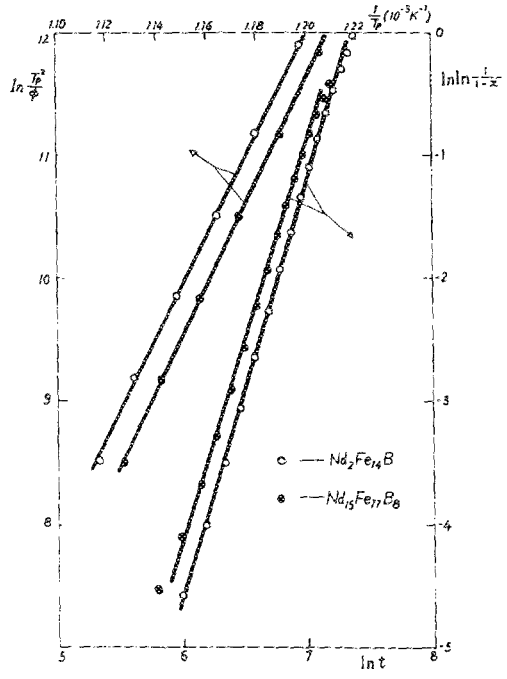

FIG. 2. Kissinger (upper lines) and Avrami (lower lines) plots for a-$Nd_2Fe_{14}B$ (open symbols) and a-$Nd_{15}Fe_{77}B8$ (solid symbols).

excess Nd and B in a-$Nd_{15}Fe_{77}B_8$ do not appear to affect the early stages of crystallization. The isochronal DSC scans, however, show significantly different behavior, as is shown in Fig. 3. The curve for $Nd_2Fe_{14}B$ is symmetrical, as expected for a polymorphic reaction. That for $Nd_{15}Fe_{77}B_8$ shows a high-temperature tail, resolved at low scan rates into a separate peak. The activation energy for this peak is identical to that of the main DSC peak. This suggests that this transformation may be due to different regions of the ribbon crystallizing at different times rather than the formation of a second phase. The tail may be drastically reduced by etching off a thin ($\approx 5\,\mu$m) layer from the surface of the ribbon, confirming our interpretation. Similar effects have been reported by Greer[5] on a-$Fe_{80}B_{20}$, where it is suggested that because of the dynamics of the melt puddle, a thin layer close to the wheel is quenched much faster than the rest of the sample

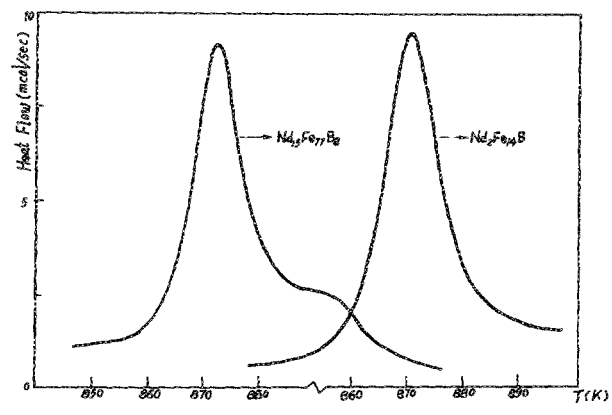

FIG. 3. DSC traces for a-$Nd_{15}Fe_{77}B_8$ and a-$Nd_2Fe_{14}B$ showing the high-temperature tail on the former sample. The curves have been displaced horizontally for clarity.

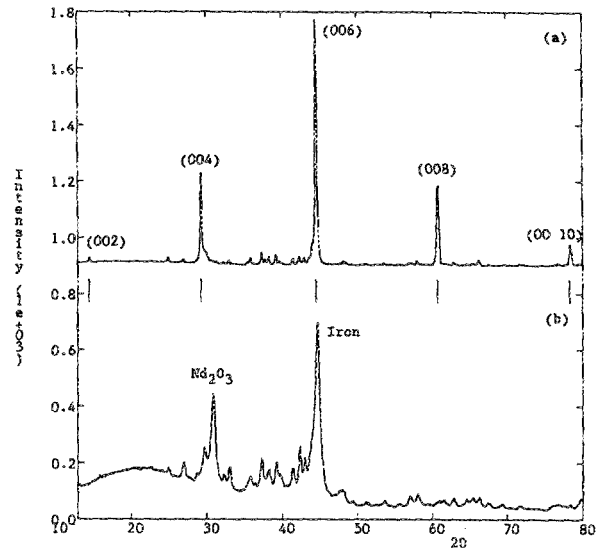

FIG. 4. X-ray diffraction scans for $Nd_2Fe_{14}B$ showing (a) a textured material and (b) a material which has oxidized.

and so has fewer nuclei. It is unclear why this effect is seen only in $Nd_{15}Fe_{77}B_8$ and not in $Nd_2Fe_{14}B$. The crystallization enthalpy for both compositions is 5.1 ± 0.1 kJ/mole.

A key question in the formation of Nd-Fe-B is whether the material may be textured, particularly whether the crystals may be grown with the c axis (the easy axis of magnetization) perpendicular to the ribbon surface. For slow quenches (less than 15 m/s), where the material is almost fully crystalline, there is a phenomenal texturing: on the wheel side *only* crystals with the c axis perpendicular to the surface are seen, as is illustrated in Fig. 4(a). Similar results have been reported by Coehoorn,[6] except that he reports texturing on the free side. We have not yet determined how deeply the texturing extends into the bulk. Crystallization of fully amorphous samples also leads to some texturing, but much less pronounced than in the partly amorphous materials. This is shown in Fig. 5, where the enhanced (0 0 2l)

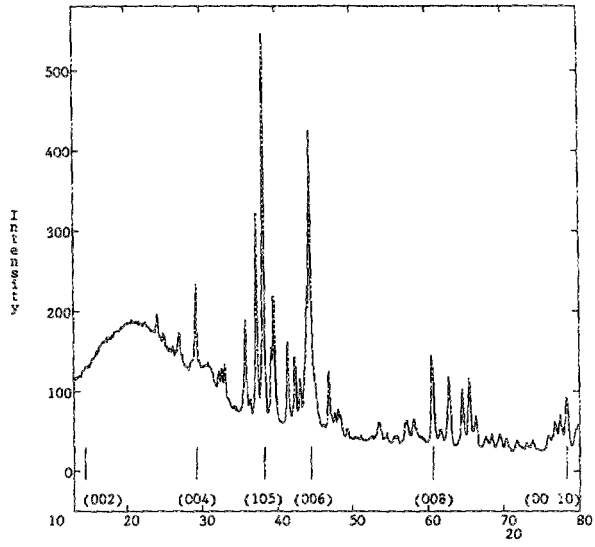

FIG. 5. X-ray diffraction scan for recrystallized $Nd_{15}Fe_{77}B_8$ showing some texturing. The broad peak centered at $2\theta \approx 20°$ is due to the sample holder.

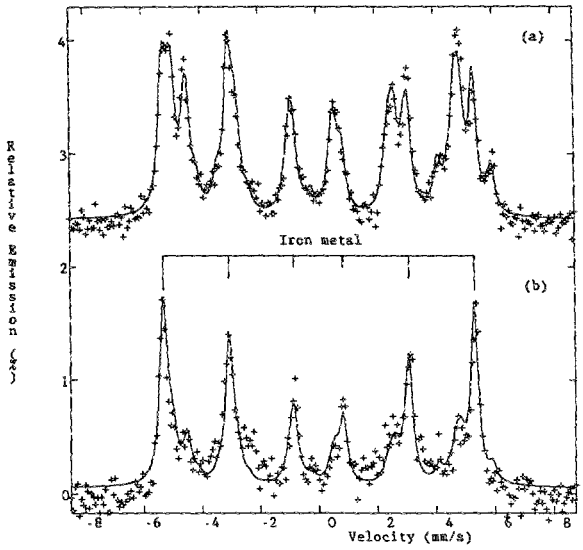

FIG. 6. Room-temperature conversion electron Mössbauer spectra for two samples of $Nd_2Fe_{14}B$ (corresponding to the samples in Fig. 4) showing (a) a surface composed mainly of $Nd_2Fe_{14}B$ and (b) mainly α-iron.

peaks are indicated. The origin of this texturing is unclear, but it may reflect internal stresses from the quenching process.

In addition to this genuine texture, effects sometimes appear which are similar in appearance but are in fact due to surface oxidation. Figure 4(b) shows the x-ray diffraction scan of $Nd_{15}Fe_{77}B_8$ which exhibits peaks at the positions corresponding to the (004) and (006) reflections of $Nd_2Fe_{14}B$. While this appears similar to the textured material in Fig. 4(a), the absence of the (002) and (008) reflections combined with the intensities of the other reflections clearly indicates that we are not dealing with textured $Nd_2Fe_{14}B$. The apparent enhancement of the (004) reflection is in fact caused by the presence of a surface layer of hexagonal Nd_2O_3 (P3ml, JCPDS #6-408) which has its principal line at the same angle. Precipitation of α-iron formed by the oxidation of $Nd_2Fe_{14}B$ leads to a contribution which overlaps with the (006) reflection of $Nd_2Fe_{14}B$. This interpretation is confirmed by CEMS shown in Fig. 6. The two spectra correspond to the two materials in Fig. 4. In order to obtain estimates of the surface composition, the data were analyzed as the sum of standard $Nd_2Fe_{14}B$ and α-Fe subspectra and only the relative areas of the two components were allowed to vary. The surface of the truly textured sample consists of mainly $Nd_2Fe_{14}B$ (over 70%), whereas that of the sample showing only enhanced (004) and (006) reflections is more than 60% α-iron.

[1]J. J. Croat, J. F. Herbst, R. W. Lee, and F. E. Pinkerton, Appl. Phys. Lett. **44**, 148 (1984).
[2]H. Fukunaga, K. Ihara, and K. Narita, IEEE Trans. J. Magn. Jpn. TJMJ-1, 998 (1985).
[3]H. Hatta, Y. Masuda, and T. Mizoguchi, IEEE Trans. J. Magn. Jpn. TJMJ-1, 1009 (1985).
[4]In a Kissinger plot, taken from an isochronal DSC scan, $\ln \phi/T_x^2$ is plotted against T_x (ϕ is the heating rate and T_x is the peak of the crystallization event); the slope yields the activation energy E_a. In an Avrami plot, taken from an isothermal scan, $\ln \ln 1/(1-x)$ is plotted against $\ln t$ (x is the fraction of material that has crystallized and t is the time); the slope yields the Avrami number, n, which characterizes the reaction.
[5]A. L. Grear, Acta Metall. **30**, 171 (1982).
[6]R. Coehoorn, Proceedings of the Sixth International Conference on Rapidly Quenched Metals, Montreal, Canada (1987).